Hydrodynamic Properties of a Double-Helical Model for DNA

J. Garcia de la Torre, S. Navarro, and M. C. Lopez Martinez
From the Departamento de Quimica Fisica, Universidad de Murcia, 30071 Murcia, Spain

ABSTRACT The translational and rotational diffusion coefficients of very short DNA fragments have been calculated using a double-helical bead model in which each nucleotide is represented by one bead. The radius of the helix is regarded as an adjustable parameter. The translational coefficient and the perpendicular rotation coefficient agree very well with experimental values for oligonuclotides with 8, 12, and 20 base pairs, for a single value of the helical radius of about 10 Å. We have also calculated a nuclear magnetic resonance relaxation time in which the coefficient for rotation about the main axis is involved. As found previously with cylindrical models, the results deviate from experimental values, indicating that the internal motion of the bases has a remarkable amplitude. An attempt to quantify the extent of internal motions is presented.

INTRODUCTION

Most dynamic properties of long DNAs are dominated by the contour length and the bending flexibility of the macromolecule, whereas the thickness and, particularly, the detailed cross-sectional structure are less important. Consequently, the solution properties of DNA have been interpreted customarily in terms of a model with wormlike contour and uniform, circular cross-section (Bloomfield et al., 1974). If the contour length of the DNA is shorter than its persistence length (this happens when the number of base pairs is roughly <100), the macromolecular filament is essentially rigid and straight, and the cross-section becomes more important. In that case the wormlike model reduces to a straight, circular cylinder. Monodisperse, short fragments of DNA of that length are becoming easily available, and can be characterized by means of hydrodynamic techniques like sedimentation (Kovacic and Van Holde, 1977), transient electric dichroism (Dieckman et al., 1982), birefringence (Lewis et al., 1986), and dynamic light scattering (Eimer and Pecora, 1991).

Using early results from those techniques, we showed (Tirado et al., 1984) that the Tirado-Garcia de la Torre theory for straight, rigid cylinders (Tirado and Garcia de la Torre, 1979, 1980; Garcia de la Torre et al., 1984) provides a consistent framework for analyzing hydrodynamic properties of DNA fragments from about 50 to 100 base pairs. More recently, Eimer and Pecora (1991) have been able to measure properties of oligonucleotides as short as 8 base pairs, finding that the Tirado-Garcia de la Torre equations for cylinders are remarkably valid for such short DNA pieces. Therefore, the cylindrical model (with a rigorous hydrodynamic treatment) provides an adequate treatment of the influence of the thickness of the DNA double helix on the hydrodynamic properties which describe the overall translational and rotational dynamics of the macromolecule, and this happens in the whole range of lengths. One may think that the details of the double-helical structure are unimportant in the description of such overall properties. One simple argument to explain this situation is that those details are somehow buried by hydration, which fills in part the grooves of the helix.

Aside from the adequacy of the cylindrical model, we think that it is important to test more detailed models that embody the helical structure of DNA, and particularly a bead model in which each nucleotide is replaced by a spherical element. In the early years of bead-model theory (Bloomfield et al., 1967; Garcia de la Torre and Bloomfield, 1977), it was thought that the beads in the model should be of macromolecular size (i.e., various orders of magnitude larger than the solvent molecules) to guarantee the validity of the continuum hydrodynamics in which the theory is based. However, bead models at a molecular scale, even with atomic resolution, were later used successfully for various biopolymers (Venable and Pastor, 1988; Porschke and Antosiewicz, 1990; Tirado et al., 1990). Indeed, the possibility of a bead model with high resolution for DNA, that would take into account the double-helical structure, was presented years ago (Garcia de la Torre and Horta, 1976, 1977), but unfortunately, experimental data on short DNA oligomers were not available by that time, and the theory was in its earliest stages.

The overall dynamics (translational and rotational diffusivity) of a piece of DNA is interesting to describe some phenomena and for characterization purposes. However, the internal dynamics may be more relevant for many aspects of DNA function. Molecular dynamics simulation, in which the elements in the model are the individual atoms, provides an insight in the fast, short-range dynamics of DNA. However, this technique cannot reach the slower, larger scale internal motions that are denoted generically as bending, torsion, or twisting. For such problems, stochastic or Brownian dynamics simulation has to be employed, with models having fewer, larger elements, but still including as much structural detail. Helical bead models are promising for that purpose. However, such models must be parameterized and tested for overall properties. This need provides the second main reason for the work reported in this article.

Received for publication 18 June 1993 and in final form 2 February 1994.
Address reprint requests to Dr. Garcia de la Torre.

0006-3495/94/05/1573/07 $2.00

THEORY AND METHODS

Helical geometry and bead models

The geometry of a single helix can be described by the following set of quantities: A, radius of the helix; P, pitch; n_t, number of turns (not necessarily integer). If the helical axis is z, then the parametric equations of the helix can be written as

$$x = A\cos(t + \phi) \qquad y = A\sin(t + \phi) \qquad z = Pt/2\pi \tag{1}$$

where the value of the phase angle, ϕ, can be arbitrary. t is a continuous parameter that goes from $t = 0$ to $t = 2\pi n_t$. The two strands of a double helix can also be described by Eq. 1, using different values for the phase angle of each strand. If we set $\phi_1 = 0$, then ϕ_2 would measure the phase difference. The most symmetric situation is that corresponding to $\phi_2 = \pi$.

In the bead model of the helix, beads of radius σ are placed along the contour of the helical line. A convenient way of expressing the density of beads is the number of beads per turn, n. In a double helix, the number of bead pairs is $N_{bp} = nn_t$ and the number of beads, N_b, would be twice this quantity. The cartesian coordinates of the beads in one strand, with bead indices $i = 0, \ldots, N_{bp} - 1$, can be obtained from Eq. 1, using instead of t the discrete parameter

$$t_i = 2\pi i/n. \tag{2}$$

For the beads in the second strand, with indices $i = N_{bp}, \ldots, 2N_{bp} - 1$, we may use the same formulas, but replacing i by $i - N_{bp} - 1$ in Eq. 2 and using the desired ϕ_2 in Eq. 1. For the symmetric double helix with $\phi_2 = \pi$, we have $x_{i-N_{bp}-1} = -x_i$, $y_{i-N_{bp}-1} = -y_i$, and $z_{i-N_{bp}-1} = z_i$.

Next, the bead radius has to be chosen. In principle, this quantity can be variable, and bead overlapping can be allowed. However, it is known that in bead model calculations, the results depend on bead radius much less than on the number and position of the beads. Therefore, to avoid an additional model parameter, we assume touching beads. Thus, there are two geometrical restrictions on the bead model. One is that the pitch cannot be smaller than the diameter of the beads, so that $P > 2\sigma$. The second one is that the distance between beads that are neighbors along the strand, u, given by

$$u = (2A^2(1 - \cos(2\pi/n)) + (2\pi/n)^2)^{1/2} \tag{3}$$

must be equal or larger than the diameter of the beads. The case of touching neighbor beads corresponds to $\sigma = u/2$. In Fig. 1 two double helix with $N_b = 15$, $A = 10$ Å, $P = 34$ Å are plotted. One of them is symmetric ($\phi = 180°$), with two equal grooves, whereas the other ($\phi = 120°$) shows two grooves of different widths.

Hydrodynamic coefficients and calculations

The hydrodynamic coefficients and other properties of the helical models have been calculated using the conventional procedure for bead models. The theory and computational procedure can be found in reviews (Garcia de la Torre and Bloomfield, 1981; Garcia de la Torre, 1989). The computer software HYDRO (Garcia de la Torre et al., 1993) was used in the calculations.

It should be pointed out that the conventional bead-model procedures are not still completely rigorous. Although the procedure includes theoretical refinements such as a rotational correction from bead size (Garcia de la Torre and Rodes, 1983; Garcia de la Torre, 1989), which is relevant for axial rotation, it still omits some hydrodynamic effects like couplings between translation and rotation at the level of individual beads, and higher order and multibody hydrodynamic interactions. However, it is usually assumed that the influence of such effects is small, hopefully <3% for models that are not too compact. Therefore the conclusions drawn from the comparison of helical models with cylindrical models and experimental data should not be affected by such effects.

The translational properties (diffusion and sedimentation) of the particle are simply determined by the translational diffusion coefficient, D_t. The complete description of the rotational diffusivity of an arbitrary particle is contained in the rotational diffusion tensor, $\mathbf{D}_r$ (Wegener et al., 1979; Garcia de la Torre, 1981). The time decay or frequency dependence of electro-optical or spectroscopic properties involves up to five rotational relaxation times (Garcia de la Torre, 1981) which can be calculated in terms of the trace, D, and anisotropy, Δ, of the $\mathbf{D}_r$ tensor, that are given by

$$D = (D_1 + D_2 + D_3)/3 \tag{4}$$

$$\Delta = (D_1^2 + D_2^2 + D_3^2 - D_1D_2 - D_1D_3 - D_2D_3)^{1/2} \tag{5}$$

where the eigenvalues of $\mathbf{D}_r$ are denoted (in increasing order) as D_1, D_2, and D_3. The expressions for the relaxation times are:

$$\tau_1 = (6D - 2\Delta)^{-1} \qquad \tau_2 = (3(D_1 + D))^{-1} \qquad \tau_3 = (3(D_2 + D))^{-1}$$
$$\tau_4 = (3(D_3 + D))^{-1} \qquad \tau_5 = (6D_1 + 2\Delta)^{-1}. \tag{6}$$

The longest relaxation time, τ_1, usually dominates the observed dynamics.

It is pertinent to recall the form of the hydrodynamic properties for the special situation of a symmetric top, i.e., a particle having an axis of symmetry. Such is the simple case of a rodlike cylinder, on which the analysis of Eimer and Pecora (1991) was based. For a straight cylinder, with the cylindrical axis along z, the $\mathbf{D}_r$ tensor is diagonal, with $D_1 = D_2 = D_{r,xx} = D_{r,yy} \equiv D_\perp$ and $D_3 = D_{r,zz} \equiv D_\parallel$. In such cases, there are distinct relaxation times, given by

$$\tau_a = (6D_\perp)^{-1} \qquad \tau_b = (5D_\perp + D_\parallel)^{-1} \qquad \tau_c = (2D_\perp + 4D_\parallel)^{-1}. \tag{7}$$

For a prolate cylinder, $D_\perp < D_\parallel$, and $\tau_1 \equiv \tau_a$, $\tau_2 = \tau_3 \equiv \tau_b$, $\tau_4 = \tau_5 \equiv \tau_c$, whereas for an oblate cylinder, $D_\perp > D_\parallel$, and $\tau_5 \equiv \tau_a$, $\tau_4 = \tau_3 \equiv \tau_b$, and $\tau_2 = \tau_1 \equiv \tau_c$.

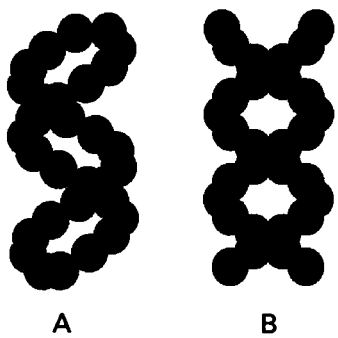

FIGURE 1 (*A*) Double-helical bead model for DNA, with $\phi = 180°$ (symmetric case). (*B*) The same, with $\phi = 120°$.

RESULTS

Comparison of models

The study of the double-helical model is directly intended to analyze solution properties of DNA. Therefore, from the beginning we set some geometrical parameters roughly equal to those of the B form of DNA. Namely, we take a pitch, $P = 34$ Å, and a number of base pairs per turn, $n = 10$. Therefore, we neglect any sequence dependence as well as bends, because both effects must be unimportant for such DNA pieces. The radius A is regarded as a variable, adjustable parameter.

As a preliminary question, we studied the dependence of the hydrodynamic properties on the angle ϕ that measures the phase shift between the two strands. The results, for a DNA dodecamer model, with plausible values of the geometrical parameters, are listed in Table 1 as a function of ϕ, which is varied from 180°, corresponding to the symmetric double helix. As ϕ is decreased, the width of one of the helix grooves

TABLE 1 Properties of a DNA model, 12 base pairs long, with A = 10 Å and P = 34 Å, and a varying phase angle between the two helices, ϕ

ϕ, °	R_g, Å	$D_t \times 10^{-7}$, $cm^2\ s^{-1}$	$\tau_{longest} \times 10^9$ s	$\tau_{shortest} \times 10^9$ s
180	15.7	13.5	6.66	4.74
165	15.7	13.5	6.65	4.72
150	15.6	13.6	6.61	4.70
135	15.6	13.7	6.54	4.64
120	15.6	13.8	6.44	4.55
105	15.6	14.0	6.31	4.44
90	15.6	14.3	6.15	4.30

increases and the other decreases. The groove width in DNA is somewhat variable, depending on a variety of factors, including sequence (Boutonet et al., 1993). However, comparison of molecular models of B-DNA with bead models suggest that the real value of ϕ should be around 120° (see Fig. 1 *B*). In Table 1, ϕ has been decreased to a rather small value, 90°, for which the model looks quite unnatural.

The results in Table 1 clearly indicate that the hydrodynamic properties are essentially insensitive to the ϕ angle. The changes in properties on going from the symmetric structure (180°) to others that look closer to molecular models (120°) are of a few percent, even smaller than typical instrumental errors. Therefore the study of some aspects of the hydrodynamics of DNA could be made with a symmetric bead model (ϕ = 180°). This may be helpful for future dynamics simulations. However, for the present bead-model calculation there is no particular advantage from symmetry and for the subsequent calculations in this work we take the molecular choice, ϕ = 120°.

Another preliminary study was concerned with the behavior of the various rotational constants, looking for the proper hydrodynamic coefficient for the comparison with experimental data. For any value of N_{bp}, the rotational diffusion tensor of the double helix has the form

$$\mathbf{D}_r = \begin{pmatrix} D_{r,xx} & D_{r,xy} & 0 \\ D_{r,xy} & D_{r,yy} & 0 \\ 0 & 0 & D_{r,zz} \end{pmatrix} \qquad (8)$$

so that we can always identify $D_{r,zz} \equiv D_{\|}$, as for circular cylinders. For very short fragments (say N_{bp} = 2 – 6), the nondiagonal component $D_{r,xy}$ is of the same order as the diagonal ones. For intermediate lengths (roughly N_{bp} = 7 – 11), we find that $D_{r,xy}$ is much smaller than $D_{r,xx}$ and $D_{r,yy}$, and it is valid to take $D_\perp = (D_1 + D_2)/2 = (D_{r,xx} + D_{r,yy})/2$. For long fragments (e.g., $N_{bp} > 11$) the 1, 2, *xx*, and *yy* values are practically identical, as for cylinders, and we simply take $D_\perp = D_1 = D_{r,xx}$.

The evolution of the trend shown by the set of eigenvalues of $\mathbf{D}_r$ and the set of relaxation times as N_{bp} increases is shown in Fig. 2. For long fragments, we can appreciate that there are only two distinct rotational diffusion coefficients, and three distinct relaxation times. Therefore, we can conclude that the rotational dynamics of a double helix can be treated, to a good approximation, as that of axysimmetric particle (symmetric top).

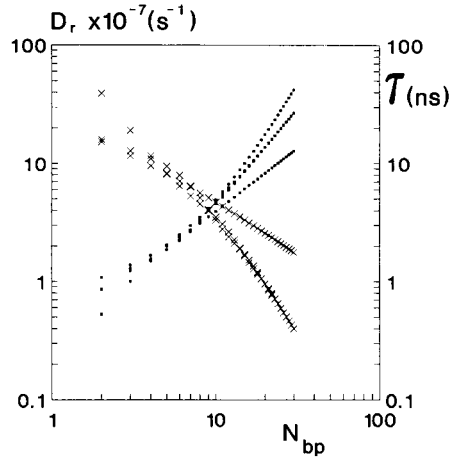

FIGURE 2 Dependence of the three rotational diffusion coefficients, $D_k(k = 1, 2, 3)(X)$ and the five relaxation times $\tau_k(k = 1, \ldots, 5)$ ■ of DNA double-helical models, on the number of base pairs, N_{bp}. The parameters of the model are A = 10 Å, P = 34 Å, and ϕ = 120°.

From the aspect of our bead models, as shown in Fig. 1, one may appreciate as an apparent deficiency that the core of the double helix (the region occupied by the planar bases) is hollow. It is well known in rigid-particle hydrodynamics that, as a consequence of hydrodynamic interaction, the innermost parts of a model have a minor contribution to the properties. Good examples of this are the results for hollow and filled cylindrical arrays of beads (Tirado and Garcia de la Torre, 1979, 1980). We have analyzed the influence of the core using a variation of the model which has more beads that fill the helix. For each nucleotide, in addition to the bead given by Eqs. 1 and 2, we use an extra bead lying on the radial direction, and tangent to the external bead at the inner side. For A = 10 Å, the radius of the external bead is σ = 3.5 Å, and we took σ' = 2.5 Å for the inner beads. Thus, 85% of the radius, A, of the helix is filled. A comparison of the results of the model with $2N_{bp}$ beads with those of the model with N_{bp} beads is presented in Table 2. We see that the effect of the core in translational diffusivity is negligible, and for rotational relaxation times, the effect is <10%. We conclude that the contribution from the core is small as expected. Although such contribution may have some marginal influence in the comparison with experimental results, we decided, for the sake of simplicity, to neglect the core adopting the model with one bead per nucleotide.

TABLE 2 Comparison of properties of the DNA model with one bead per nucleotide (A), with those of a test model with two beads per nucleotide (B). The geometric parameters are A = 10 Å, P = 34 Å, ϕ = 120, σ = 3.5 Å, and σ' = 2.5 Å

	$D_t \times 10^{-7}$, $cm^2\ s^{-1}$		$\tau_{longest} \times 10^9$ s		$\tau_{shortest} \times 10^9$ s	
N_{bp}	(A)	(B)	(A)	(B)	(A)	(B)
6	18.8	18.6	2.4	2.6	2.2	2.4
14	12.8	12.7	8.5	9.1	6.2	6.7

It is also interesting to compare the results for the helical bead model with those calculated for cylinders of length $L = PN_{bp}/n$ and diameter $2A$ using the Tirado-Garcia de la Torre equation (Tirado and Garcia de la Torre, 1979, 1980). The comparison can be performed in terms of dimensionless combinations of properties such us the $f(p)$ function, where $p = L/2A$ (Garcia de la Torre et al., 1984), which combines D_t and $D_\perp$, and the ratio of the two rotational coefficients, $D_\parallel/D_\perp$. The values of $f(p)$ for the helical model are quite close to those reported for cylinders. However, the $D_\parallel/D_\perp$ ratio behaves differently, as shown in Fig. 3. For the helical model $D_\parallel$ is appreciably smaller than for the cylinder of the same p. The plot of this ratio for the bead model can be used also to analyze the effect of the ϕ angle in the double helix. One would expect that the symmetric model might underestimate $D_\parallel$. We find that this is true, but the magnitude of the effect is very small: the $D_\parallel/D_\perp$ ratios for the symmetric and asymmetric models are nearly coincident, as seen in Fig. 3.

Comparison with experimental data

The central part of our analysis is the comparison of calculated results for the diffusion constants with experimental data of DNA, and particularly with the Eimer-Pecora data for the shortest fragments with $N_{bp} = 8$, 12, and 20, for which the details of the cross-sectional structure must be more relevant. The comparison is made in Fig. 4 for the translational diffusion coefficient, D_t, and in Fig. 5 for the rotational diffusion coefficient, $D_\perp$. Error bars of about 4% are attached to the D_t data. For $D_\perp$ the error bars are of the same size as the plotted symbols. We see that the two properties of the three fragments are well described for the double-helical model with a helix radius $A = 10$–11 Å. The fit is very good for $D_\perp$, and for D_t there seems to be a slight systematic deviation, which is of a magnitude close to the experimental errors. The agreement is nearly as good as that found by Eimer and Pecora for the cylindrical model with the Tirado-Garcia de la Torre theory. Indeed plots like Figs. 4 and 5 for cylinders (not shown) have the very same aspect, again with a somewhat better fit for $D_\perp$ than for D_t.

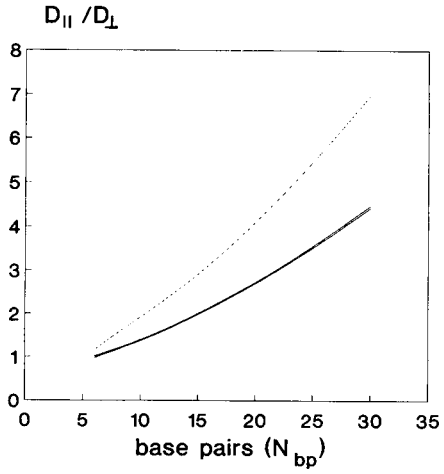

FIGURE 3 Plot of the $D_\parallel/D_\perp$ ratio as a function of length expressed as the number of basepairs ($A = 10$ Å, $P = 34$ Å). The dashed curve is for the cylinder, and the two practically coincident continuous lines are for double helices with $\phi = 180°$ and $\phi = 120°$.

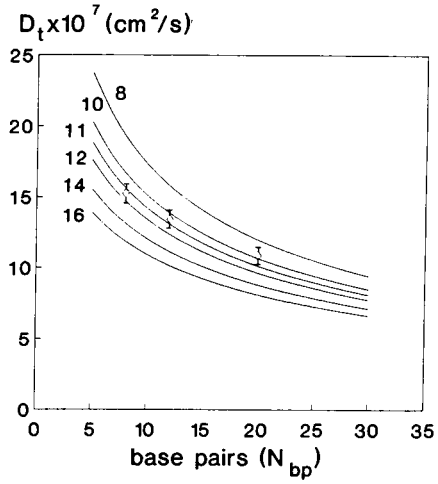

FIGURE 4 Plot of the translational diffusion coefficient, D_t, versus number of base pairs, N_{bp}. Continuous curves are calculated values for $P = 34$ Å, $\phi = 120°$, and the indicated values of the helix radius. The data points are experimental values of Eimer and Pecora (1991).

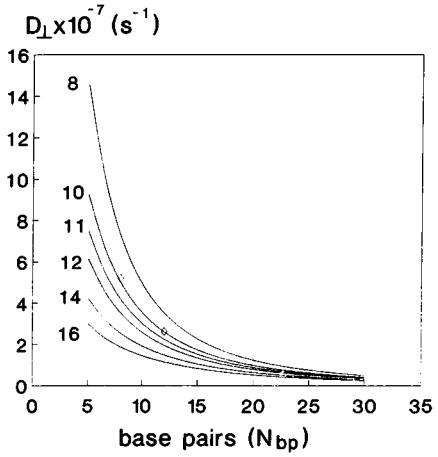

FIGURE 5 Plot of the rotational diffusion coefficient, $D_\perp$, versus number of base pairs, N_{bp}. Continuous curves are calculated values for $P = 34$ Å, $\phi = 120°$, and the indicated values of the helix radius. The data points are experimental values of Eimer and Pecora (1991).

The helix radius $A = 10$–11 Å is in turn very close to the crystallographic radius of the B-DNA helix, measured at the phosphate group. Our bead model for the double helix is actually somehow thicker due to the size of the spherical beads, that for $A = 10$ Å (from the axis to the center of the bead) is $\sigma \cong 4$ Å; its thickness (or effective radius from the axis the outer surface) ranges between A + σ at the base planes and A at a plane halfway between bases. The mean value is about 12–13 Å, with an additional amount of 2–3 Å more than the crystallographic value, that can be reasonably attributed to hydration.

The rotational diffusion coefficient for rotation around the helical axis, $D_\parallel$, can be expected to be more sensitive to the

transversal structure and size than $D_\perp$. One experimental technique that monitors the rotation around the main axis is time-resolved nuclear Overhauser effect cross-relaxation. This technique has been applied recently to short DNA fragments by various authors (Eimer et al., 1990; Birchall and Lane, 1990). From the experimental cross-relaxation rate for a pair (r, s) of protons, σ_{rs}, the nuclear magnetic resonance (NMR) relaxation time is obtained as $\tau_{nmr} = -(10r^6/\nu_H^4 h^2)\sigma_{rs}$, where ν_H is the proton gyromagnetic constant, and r is the distance between the pair of protons. For a rigid, arbitrarily shaped particle, $\tau_{nmr}^{(rb)}$ is a combination of the five relaxation times in Eq. 6. (The (rb) subscript makes reference to rigid-body behavior). For a symmetric top, such as a cylinder, τ_{nmr} is a combination of the three relaxation times in Eq. 7. The coefficients in the linear combination are functions of the orientation of the proton-proton vector in the system of reference of rotational diffusion. For the symmetric top, it just depends on the angle subtended by that vector and the particle axis. For a review of the theory, see Eimer et al. (1990) or Birchall and Lane (1990). As discussed above, the double helix is not geometrically an axisymmetric particle, but its rotational diffusion tensor has the same structure as that of a symmetric top; therefore the same equations hold.

The experimental results, reported or compiled by those authors correspond to the H5-H6 pair of cytosine, which is in the planes of bases. The proton-proton vector is then perpendicular to the axis and the NMR relaxation times takes a simpler form

$$\tau_{nmr}^{(rb)} = \frac{\tau_a}{4} + \frac{3\tau_c}{4} = \frac{1}{4}(6D_\perp)^{-1} + \frac{3}{4}(2D_\perp + 4D_\parallel)^{-1}. \quad (9)$$

Combining the values of $D_\perp$ and $D_\parallel$ calculated for our double-helical model, we have calculated the NMR relaxation time. The results for the fitted value of the double helix, $A = 10$ Å, are compared in Fig. 6 *A* with experimental results for oligonucleotides with $N_{bp} = 6$ to 20. We also include the values calculated for cylinders with a radius of 10.5 Å, which is the best fit found by Eimer and co-workers (Eimer et al., 1990; Eimer and Pecora, 1991) for the relaxation times in dynamic light scattering. As noted by these authors, there is a clear deviation of the results calculated for cylinders from the experimental values. Now we see that the calculation for the helix, again using the same radius that fit scattering, falls above the cylinder results. Analyzing the values of the two diffusion coefficients D_t and $D_\perp$, we see that results for cylinder are quite close to those for helices, but $D_\parallel$ is appreciably lower for the helix than for the cylinder. (We recall that this situation persists with the modified, filled double helix.) According to Eq. 9, $\tau_{nmr}^{(rb)}$ is higher for the helix, and deviates more from the experimental values. Strictly speaking, the agreement with measurements is worse for the helical model. However, according to Eimer et al. (1990), deviations between experimental values of $D_\parallel$ or τ_{nmr} and results for rigid models (which, on the other hand, fit well both D_t and $D_\perp$) must be expected from the torsional flexibility of the double helix, which is dynamically mixed with axial rotation. Indeed, those authors attributed entirely the deviation of the results for rigid cylinders to internal, torsional motion. If the same is assumed for the results from the double-helical hydrodynamic model, the extent of the internal motion of the bases in DNA may be even greater than that predicted in terms of a cylindrical model, as shown next.

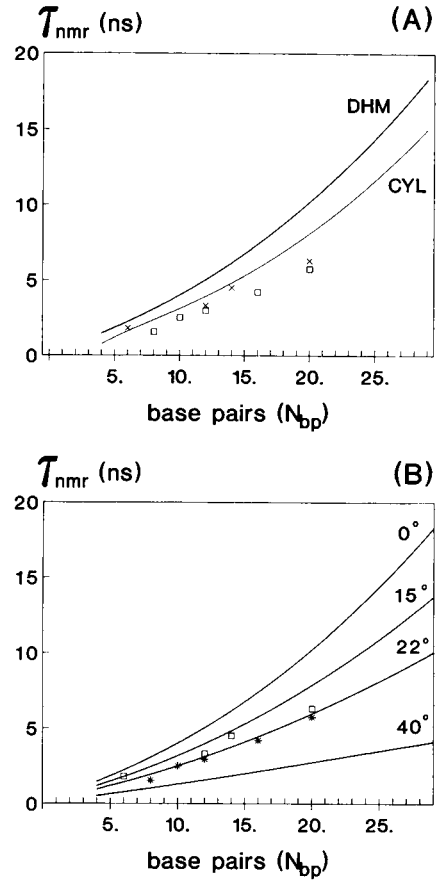

FIGURE 6 NMR relaxation time for the H5-H6 pair of cytosine versus number of base pairs. (*A*) Results for rigid models: DHM, double helical model with $P = 34$ Å, $\phi = 120°$, $A = 10$ Å; CYL, cylinder of the same diameter. The experimental data points are: *, from Eimer et al. (1990), and □, from Birchall and Lane (1990). (*B*) Results for the DHM corrected for internal motion, using the Schurr-Fujimoto theory, with the indicated values of the root-mean-square angular displacement, $\langle \delta\epsilon^2 \rangle^{1/2}$.

Analysis of internal motions

So far, we have accomplished the main purpose of our work, showing how the double-helical model, with realistic parameters, predicts very well the overall translational and rotational diffusion of short DNA fragments. In future work, the model may be complemented with some field of forces between beads, making it useful to simulate the whole dynamics of the double helix. Here, it is possible to estimate the extent of internal motion, attributing entirely to it the deviation of the calculated $\tau_{nmr}^{(rb)}$ from the experimental τ_{nmr}. This analysis has been performed by Eimer et al. (1990) using the cylinder as the rigid model. Using our results for the double-helical model, we now can investigate the model dependence of the results.

Our analysis proceeds along the same way followed by Eimer et al. (1990), using the two alternative methods and the same assumptions made by those authors. The first one is based on the model-free approach of Lipari and Szabo (1982a, b). The wobbling of the internuclear vector is characterized by a single correlation time τ_{int}. If such time is assumed to be much faster than the overall correlation time, then the correlation function is well approximated by a single exponential with correlation time

$$\tau_{nmr} = S^2\tau_{nmr}^{(rb)} + (1 - S^2)\tau_{int} \tag{10}$$

where S is the generalized order parameter, and the rigid-body correlation time, $\tau_{nmr}^{(rb)}$, is that from Eq. 9. As in the calculations of Eimer et al. (1990) we use an estimate of $\tau_{int} = 50$ ns. The extent of internal motion can be measured by parameters with more physical implication that S, but this requires that the motion is represented by a particular model. In the wobbling in a cone model (Wang and Pecora, 1980; Lipari and Szabo, 1981) the internuclear vector diffuses freely within a cone of semiangle θ_0, related to the order parameter by

$$S_{cone} = \frac{1}{2}\cos\theta_0(1 + \cos\theta_0). \tag{11}$$

The second method is based on a theory by Schurr and Fujimoto (Schurr, 1984; Schurr and Fujimoto, 1988). The intermolecular vector undergoes overdamped harmonic librations, described by angular coordinates ϵ (polar) and η (azimuthal), about an equilibrium position ϵ_0. Assuming that the internal relaxation times of the two coordinates are much shorter than the rotational relaxation times, then the observed NMR relaxation time is given by

$$\tau_{nmr} = C_0(6D_\perp)^{-1} + C_1(5D_\perp + D_\parallel)^{-1} + C_2(2D_\perp + 4D_\parallel)^{-1}. \tag{12}$$

In our case, $\epsilon_0 = 90°$, and therefore, for isotropic motion the root mean square angular displacements for the two coordinates are identical: $\langle \delta\epsilon^2 \rangle^{1/2} = \langle \delta\eta^2 \rangle^{1/2}$. Then, the constants in Eq. 12 take a particularly simple form:

$$C_0 = \frac{1}{4}\left[\frac{1}{4} - \frac{3}{2}\exp(-2\langle \delta\epsilon^2 \rangle) + \frac{9}{4}\exp(-4\langle \delta\epsilon^2 \rangle)\right] \tag{13}$$

$$C_2 = \frac{3}{16}\left[1 + 2\exp(-2\langle \delta\epsilon^2 \rangle) + \frac{1}{2}\exp(-4\langle \delta\epsilon^2 \rangle) + \frac{1}{2}\exp(-8\langle \delta\epsilon^2 \rangle)\right] \tag{14}$$

and $C_1 = 0$. It is noteworthy that, if internal motion is suppressed, $\langle \delta\epsilon^2 \rangle^{1/2} = 0$ and these results reduce to the rigid-body expression for $\tau_{nmr}^{(rb)}$, expressed in Eq. 9.

In the comparison of the outcome of the two methods, the compared values must be those of parameters with similar physical meaning, although the distribution function for the angular displacements are different qualitatively. We think that the root-mean-square angular fluctuation from the Schurr theory, $\langle \delta\epsilon^2 \rangle^{1/2}$, should be compared with the root-mean-square angle in the other theory, $\langle \theta^2 \rangle^{1/2}$, defined as

$$\langle \theta^2 \rangle = \frac{\int \theta^2 p(\theta)\sin\theta\, d\theta}{\int p(\theta)\sin\theta\, d\theta} \tag{15}$$

where for the cone model the unnormalized distribution is $p(\theta) = \sin\theta$ and the integration limits are 0 and θ_0. The involved integrals are trivial, and the result is

$$\langle \theta^2 \rangle = \frac{-\theta_0^2\cos\theta_0 + 2\theta_0\sin\theta_0 + 2\cos\theta_0 - 2}{1 - \cos\theta_0}. \tag{16}$$

To check our numerical procedures, we first reproduced the analysis of Eimer et al. (1990). Inserting in Eqs. 9 and 12 the values for $D_\perp$ and $D_\parallel$ calculated for cylinders with $d = 20.5$ Å, and using only their subset of experimental data, a least-squares minimization gives for the adjustable parameters in each method the same values, $S = 0.82$ (so that $\theta_0 = 29°$) and $\langle \delta\epsilon^2 \rangle = 18°$, which coincide with their results. For the sake of completeness, the same procedure was performed with the experimental data from Birchall and Lane (1990) and with the union of the two subsets of data. The results are listed in Table 3.

Then, the analysis was repeated for the double-helical model in the same way, now using θ_0 values calculated for double helices with radius $A = 10$ Å, $P = 34$ Å, and $\phi = 120°$. This also was performed for the three choices of experimental data. The results are listed in Table 3. Fig. 6 *B* presents, for the Schurr-Fujimoto model, the τ_{nmr} versus length curves for various values of the root-mean-square amplitude, showing the best fit. (A similar figure for the other model has the same aspect.) It was clear from the discussion of Eimer et al. (1990) that the amplitudes of the internal motions of the DNA bases are model-dependent. The differences in the influence of the model used for describing the internal dynamics may be smoothed, depending on which parameters are chosen in the comparison. This is illustrated in Table 3, where we see that the cone root-mean-square angle, $\langle \theta^2 \rangle^{1/2}$, is much closer to $\langle \delta\epsilon^2 \rangle^{1/2}$ than the other cone parameter, θ_0.

TABLE 3 Results of the analysis of τ_{nmr} in terms of internal motions, using the methods described in the text

Model	Experimental data	S	θ_0, °	$\langle\delta\theta^2\rangle^{1/2}$, °	$\langle\delta\epsilon^2\rangle^{1/2}$, °
Cylinder	Eimer et al. (1990)	0.82	29	20	18
Cylinder	Birchal and Lane (1990)	0.87	24	17	14
Cylinder	Both subsets of data	0.85	26	18	16
Double helix	Eimer et al. (1990)	0.74	35	25	24
Double helix	Birchal and Lane (1990)	0.79	31	22	21
Double helix	Both subsets of data	0.77	33	23	22

From the present work, it is evident that the evaluation of internal motion is also model-dependent in regard to the description of the overall dynamics of the molecule. Although the cylindrical and the double-helical models have the same D_t and $D_\perp$, they differ in $D_\parallel$, and this is the origin of the differences in the extent of internal motions predicted by each model. Eimer et al. (1990) estimated a root-mean-square amplitude of internal motions of about 20° using the simple, cylindrical model. They cited some measurements suggesting that internal motion can be so wide, although other authors have found a significantly smaller amplitude (Schurr and Fujimoto, 1988). From Table 3 we see that, when a double-helical model is adopted for DNA, the root-mean-square amplitudes are about 6° higher than the predictions from the cylindrical model. Although this is somehow beyond previous estimates (Eimer et al., 1990), the difference is not too large, and its significance may be tested in future works, perhaps analyzing other sets of data or other properties. Anyhow, the root-mean-square angular fluctuation of about 25° obtained in this work can be considered as a reasonable upper limit estimate of the extent of internal motion in DNA.

This work was supported by Grant PB90-0303 from Direccion General de Politica Cientifica (Ministerio de Educacion y Ciencia) and Grant PIB 93/17 from Comunidad Autonome de la Region de Murcia.

REFERENCES

Birchall, A. J., and A. N. Lane. 1990. Anisotropic rotation in nucleic acid fragments: significance for determination of structures from NMR data. *Eur. Biophys. J.* 19:73–78.

Bloomfield, V. A., D. M. Crothers, and I. Tinoco, Jr. 1974. Physical Chemistry of Nucleic Acids. Harper & Row Publishing Co., New York. 517 pp.

Bloomfield, V. A., W. O. Dalton, and K. E. VanHolde. 1967. Frictional coefficients of multisubunit structures. I. Theory. *Biopolymers.* 5: 135–234.

Boutonnet, N., X. Hui, and K. Zakrzewska. 1993. Looking into the grooves of DNA. *Biopolymers.* 33:479–490.

Dieckman, S., W. Hillen, B. Morgener, R. D. Wells, and D. Porschke. 1982. Orientation relaxation of DNA restriction fragments and the internal mobility and he double helix. *Biophys. Chem.* 15:263–270.

Eimer, W., and R. Pecora. 1991. Rotational and translational diffusion of short rodlike molecules in solution: oligonucleotides. *J. Chem. Phys.* 94: 2324–2329.

Eimer, W., J. R. Williamson, S. G. Boxer, and R. Pecora. 1990. Characterization of the overall and internal dynamics of short oligonucleotides by depolarized dynamic light scattering and NMR relaxation measurements. *Biochemistry.* 29:799–811.

Garcia de la Torre, J. 1981. Rotational diffusion coefficients. *In* Molecular Electro-Optics. S. Krause, editor. Plenum, New York, 75–103.

Garcia de la Torre, J. 1989. Hydrodynamic properties of macromolecular assemblies. *In* Dynamic Properties of Biomolecular Assemblies. S.E. Harding and A. Rowe, editors. Royal Society of Chemistry, Cambridge. 1–41.

Garcia de la Torre, J., and V. A. Bloomfield. 1977. Hydrodynamic properties of macromolecular complexes. I. Translation. *Biopolymers.* 16: 1747–1763.

Garcia de la Torre, J., and V. A. Bloomfield. 1981. Hydrodynamic properties of complex, rigid, biological macromolecules. Theory and applications. *Q. Rev. Biophys.* 1981:81–139.

Garcia de la Torre, J., and A. Horta. 1976. Sedimentation coefficient and x-ray scattering of double helical model for DNA. *J. Phys. Chem.* 80: 2028–2035.

Garcia de la Torre, J., and A. Horta. 1977. Anisotropic light scattering from the rigid structure of DNA. *Polymer J.* 9:33–39.

Garcia de la Torre, J., M. C. Lopez Martinez, and M. M. Tirado. 1984. Dimensions of short rodlike macromolecules from translational and rotational diffusion coefficients. Study of the gramicidin dimer. *Biopolymers.* 23:611–615.

Garcia de la Torre, J., S. Navarro, M. C. Lopez Martinez, F. G. Diaz, and J. J. Lopez Cascales. 1993. HYDRO User Manual. University of Murcia.

Garcia de la Torre, J., and V. Rodes. 1983. Effects from bead size and hydrodynamic interactions on the translational and rotational coefficients of macromolecular bead models. *J. Chem. Phys.* 79:2454–2460.

Kovacic, R. T., and K. E. VanHolde. 1977. Sedimentation of homogeneous double stranded DNA molecules. *Biochemistry.* 16:1490–1498.

Lewis, R. J., R. Pecora, and D. Eden. 1986. Transient electric birefringence measurements of the rotational and internal bendin modes in monodisperse DNA fragments. *Macromolecules.* 19:134–139.

Lipari, G., and A. Szabo. 1981. Pade approximants to correlation functions for restricted rotational diffusion. *J. Chem. Phys.* 75:2971–2976.

Lipari, G., and A. Szabo. 1982a. Model-free approach to the interpretation of nuclear magnetic resonance relaxation in macromolecules. 1. Theory and range of validity. *J. Am. Chem. Soc.* 104:4546–4559.

Lipari, G., and A. Szabo. 1982b. Model-free approach to the interpretation of nuclear magnetic resonance relaxation in macromolecules. 2. Analysis of experimental results. *J. Am. Chem. Soc.* 104:4559–4570.

Porschke, D., and J. Antosiewicz. 1990. Permanent dipole moment of tRNA's and variation of their structure in solution. *Biophys. J.* 58: 403–411.

Schurr, J. M. 1984. Rotational diffusion of deformable macromolecules with mean local cylindrical symmetry. *Chem. Phys.* 84:71–96.

Schurr, J. M., and B. S. Fujimoto. 1988. The amplitude of local angular motions of intercalated dyes and bases in DNA. *Biopolymers.* 27: 1543–1569.

Tirado, M. M., and J. Garcia de la Torre. 1979. Translational friction coefficients of rigid, symmetric top macromolecules. *J. Chem. Phys.* 71: 2581–2587.

Tirado, M. M., and J. Garcia de la Torre. 1980. Rotational dynamics of rigid, symmetric top macromolecules. *J. Chem. Phys.* 73:1986–1993.

Tirado, M. M., M. C. Lopez Martinez, and J. Garcia de la Torre. 1984. Comparison of theories for the translational and rotational diffusion coefficients of rodlike Monte Carlo. Application to short rodlike cylinders. *J. Chem. Phys.* 81:2047–2052.

Tirado, M. M., M. A. Jimenez, and J. M. Garcia Bernal. 1990. Translational diffusion and intrinsic viscosity of globular proteins. Theoretical predictions using hydrated hydrodynamic models. Applications to BPTI. *Int. J. Biol. Macromol.* 12:19–24.

Venable, R. M., and R. Pastor. 1988. Frictional models for stochastic simulations of proteins. *Biopolymers.* 27:1001–1004.

Wang, C. C., and R. Pecora. 1980. Time-correlation functions for restricted rotational diffusion. *J. Chem. Phys.* 72:5333–5340.

Wegener, W. A., R. M. Dowben, and V. J. Koester. 1979. Diffusion coefficients for segmentally flexible macromolecules: general formalism and application to rotational behavior of a body with two segments. *J. Chem. Phys.* 70:622–632.